

Paracrystalline microdomains in monatomic liquids. II. Three-dimensional structure of microdomains in liquid lead

B. Steffen and R. Hosemann

Teilinstitut für Strukturforschung am Fritz-Haber-Institut der Max-Planck-Gesellschaft, Berlin-Dahlem, Germany

(Received 14 May 1975)

The radial density function of liquid lead observed at 350, 450, and 550°C can be synthesized by a three-dimensional convolution polynomial. In contrast to other averaging methods ours enables one to obtain direct information about the three-dimensional structure of the paracrystalline microdomains. These microdomains can be quantitatively described by a face-centered arrangement of bimodal coordination statistics. Their centers of gravity are at the same distance from the reference atom as when below the melting point. The weight of the coordination statistics gives the coordination number. We find that this diminishes at the melting point from 12 to $K = 11.6 \pm 0.2$. We can explain this decrease by Schottky and Frenkel defects. In addition to this decrease we observed that the volume of fluctuation of the coordination statistics is six times larger. From these two observations and from a consideration of the shape of the coordination statistics one obtains some information concerning the diffusion of the vacancies and the one- and two-dimensional collective motions of the atoms to interstitial sites. Furthermore, the statistics were found to be bimodal. One component corresponds to intraparticle distances which are smaller than in the solid state. The other component corresponds to interparticle distances, which can be attributed to semidislocations and other distortions as, for example, grain boundaries. In the conventional theories of liquids only spherically symmetric (one-dimensional) functions are applied to average the microdomains. Here we point out that such one-dimensionally defined "direct correlation functions" and pair potentials hide the real nature of the short-range order.

I. INTRODUCTION

It was the idea of Ornstein and Zernike¹ that in a monatomic liquid each atom should be *a priori* surrounded in a similar manner. From this they developed the concept of the "direct correlation function" $c(\vec{r})$ defined by the equation

$$h(\vec{r}) = c(\vec{r}) + \rho_0 \int c(\vec{r}') h(\vec{r}' - \vec{r}) d^3r', \quad (1)$$

with $h(\vec{r}) = g(\vec{r}) - 1$. ρ_0 is the mean number density of the centers of the atoms and $g(r)$ is their radial density distribution, which gives the probability of finding an atom at a distance r from an arbitrarily chosen atom in the melt, divided by ρ_0 .

Under the assumption that both $h(\vec{r})$ and $c(\vec{r})$ are spherically symmetric the evaluation of the Fourier transform of Eq. (1) gives the one-dimensional function $c(\vec{r})$ from measured intensity values.²⁻⁴ The fact that these authors of Refs. 2-4 get direct correlation functions, which oscillate only for liquid metals and not for liquid noble gases, is interpreted by them as a result of oscillating pair potentials. We believe, however, that such oscillations may have no physical significance and result from the arbitrary introduction of spherical symmetry.

We will show in this work that this spherical symmetry is not present in the short-range atomic arrangement in liquid lead and furthermore, that the structure of molten lead can be described as a distorted fcc lattice and that the probability that nearest neighbors be found on fcc-lattice points is still about five times larger, as should

be expected from a spherically symmetric distribution.

This can easily be understood if one takes into account that the function $g(\vec{r})$ defined in Eq. (1) is nothing more than the convolution square of the instantaneous density distribution $\rho(\vec{r})$ of the centers of the atoms,^{5,6}

$$\rho_0 g(\vec{r}) = \int \rho(\vec{r}') \rho(\vec{r}' - \vec{r}) d^3r', \quad \rho_0 = \langle \rho(\vec{r}) \rangle. \quad (2)$$

All of the microdomains of $\rho(\vec{r}')$ with distorted lattice arrays are superimposed in Eq. (2) onto a convolution function $g(r)$, which is spherically symmetric only to within the experimental errors.

There have been many attempts to describe the structure of simple liquids as distorted solid-state lattices⁷ or as aggregations of microparacrystallites, which are lattices with liquidlike distortions.^{8,9} In the case of metals with a close-packed solid-state lattice such attempts resulted in synthetic density distributions with a distance ratio of second to first maximum of $1.73 = \sqrt{3}$. The measured value for molten metals, however, is always greater than 1.8 and in liquid lead it is 1.9. These discrepancies caused many authors to think that the liquid structure is very different from the solid one, as for example, the random packing proposed by Bernal.⁸ However, such models unfortunately give a mean density ρ_0 for liquid metals that is much too small.

It will be shown that the model of a paracrystalline distorted fcc lattice gives correct results for

the radial distribution function if the calculations are performed three dimensionally.

II. PARACRYSTALLINE DISTORTIONS IN fcc LATTICES

The concept of the paracrystal⁵ is based upon the assumption that for each atom in the melt there is the same probability of finding a certain surrounding. So far this resembles the ideas of Zernike and Ornstein,¹ where $h(r)$ is built up by the so-called direct correlation function, which in all published examples is spherically symmetric. The concept of paracrystallinity requires a convolution polynomial, which describes a three-dimensional distorted lattice which is clearly not spherically symmetric. The coordination vectors correspond to the so-called coordination statistics and describe the probability of finding a nearest neighbor. In the case of molten lead one finds that this lattice can be understood and is related to a face-centered cube. Attempts to use a bcc lattice failed.^{9,10} At this moment we cannot exclude hcp lattices with stacking faults.¹¹

As far as possible the uncertainty in expressing our result for a fcc lattice is defined by six statistical parameters and their standard deviations.) (The accuracy of these parameters cannot yet be given. However, we are attempting to devise a computer program to assess the reliability of the solution.) When starting from a fcc lattice we need only describe a $\frac{1}{48}$ part of the space. Figure 1 shows such a part together with the coordination statistics of four nearest neighbors. Assuming the lattice constant has length 2, in the ideal fcc lattice the atoms have to lie on positions U, V, W , where

$$U + V + W = 2n \quad (U, V, W, n: 0, 1, 2, 3, \dots), \quad (3)$$

and we obtain for the special $\frac{1}{48}$ part of Fig. 1 the conditions

$$U \geq V \geq W \geq 0. \quad (4)$$

The coordination numbers K of equivalent atoms [permutations of (UVW) which give these equivalent positions] are

$$\begin{aligned} K &= 48, & \text{for } U > V > W > 0, \\ K &= 24, & \text{for } U > V, \text{ and } W = 0 \text{ or } U = V \text{ and } W \neq 0, \\ K &= 12, & \text{for } U = V \text{ and } W = 0, \\ K &= 8, & \text{for } U = W, \\ K &= 6, & \text{for } V = 0. \end{aligned} \quad (5)$$

$H_{(1)}$, $H_{(2)}$, $H_{(3)}$, and $\hat{H}_{(3)}$ in Fig. 1 symbolize the coordination statistics of the atoms at the positions 011, 101, 110, and $\bar{1}\bar{1}0$, while the center of the cubic cell lies at 000. They all have the same shape $H(\vec{r})$ for reasons of symmetry, but are turned into the different directions $[011]$, $[101]$,

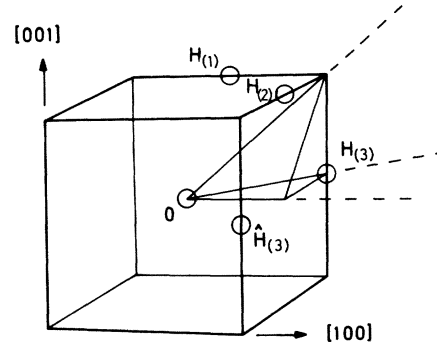


FIG. 1. Four first-neighbor coordination statistics, which expand $\frac{1}{48}$ of the paracrystalline convolution-distorted fcc lattice.

$[110]$, and $[\bar{1}\bar{1}0]$ and are normalized to unity,

$$\int H(\vec{r}) d^3\vec{r} = 1.$$

Let us consider what the distance statistics of the non-nearest neighbors $H(2, 1, 1)$ look like. Since we have assumed that the coordination statistics of the nearest neighbors shall be the same for all atoms for reasons of statistical symmetry, the 211 atom must have the same statistics with respect to the 110 atom as the 101 atom has with respect to the 000 atom, namely $H_{(2)}$. The 110 atom has the statistic $H_{(3)}$ with respect to the 000 atom. Thus when looking from the atom at the origin, the 211 atom must have the statistic

$$\begin{aligned} H(2, 1, 1) &= H_{(2)} * H_{(3)} \\ &= \int H_{(2)}(\vec{y}) H_{(3)}(\vec{x} - \vec{y}) d^3\vec{y}. \end{aligned} \quad (6)$$

$H_{(2)} * H_{(3)}$ is called the convolution product of $H_{(2)}$ and $H_{(3)}$. It follows *a priori* from the definition of the same distance statistic for all atoms that the number of convolutions of $H_{(1)}$, $H_{(2)}$, $H_{(3)}$, and $\hat{H}_{(3)}$ in order to get the statistic at UVW is given by the minimum total number of steps required to go from 000 to UVW in the direction of nearest neighbors. If p_v are the folding powers of the $H_{(v)}$ for the statistic at UVW , the final equation is

$$\begin{aligned} H(U, V, W) &= \delta(\vec{r}) * H_{(1)} * \dots * H_{(1)} * H_{(2)} * \dots * H_{(2)} \\ &\quad * \dots * H_{(3)} * \dots * \hat{H}_{(3)} * \dots * \hat{H}_{(3)}, \end{aligned} \quad (7)$$

where $\delta(\vec{r})$ is the Dirac function and $H_{(n)}$ ($\hat{H}_{(3)}$) appears p_n (\hat{p}_3) times. The calculated $H(U, V, W)$ now must be multiplied with the coordination number of Eq. (5); all statistics must then be summed. These are a special type of convolution polynomials $z_1(\vec{r})$ which are defined by the theory of paracrystals,^{5,6}

$$z_1(\vec{r}) = \sum_{UVW} K_{UVW} H(U, V, W). \quad (8)$$

This three-dimensional function is integrated over a sphere of radius r and gives the function $g(r)$ of Eq. (1),

$$4\pi r^2 \rho_0 g(r) = \int_{r=\text{const}} z^1(\vec{r}) d^3\vec{r}. \quad (9)$$

Now the coordination statistics $H_{(1)}, H_{(2)}, H_{(3)}$ are varied until the observed radial distribution function is fitted. The K_{UVW} are defined by Eq. (5) for the undistorted crystalline lattice. Vacancies are taken into account by replacing the $H_{(n)}$ in Eq. (7) by $\gamma H_{(n)}$. Then

$$K'(0, 1, 1) = \gamma K(0, 1, 1) \quad (10)$$

is the coordination number of next-nearest-neighbor statistics. The analysis of the direct correlation function $c(r)$ in Eq. (1), which gives

$$c(r) = \int_{r=\text{const}} \sum H_{(n)}(\vec{r}) d^3\vec{r}, \quad (11)$$

will be discussed in a future publication.

From Fig. 1 one perceives that all atoms within a lattice plane $W=0$ can be attained by convolution products of $H_{(3)}$ and $\hat{H}_{(3)}$ coordination statistics. The lattice plane $W=\text{const}$ can be reached by W convolutions of $H_{(1)}$ and/or $H_{(2)}$; hence

$$p_1 + p_2 = W. \quad (12)$$

Furthermore, one has to take into account the fact that

$$(1, \bar{1}, 0) + (0, 1, 1) = (1, 0, 1). \quad (13)$$

All products $H_{(1)} * \hat{H}_{(3)}$ which appear in the convolution polynomial must therefore be replaced by $H_{(2)}$, since a minimum number of steps must be used. One can calculate all distance statistics $H(U, V, W)$ using simple rules. $H(5, 1, 0)$, for example, is given by $p_3 = 3, \hat{p}_3 = 2$; $H(5, 2, 1)$ by $p_2 = 1, p_3 = 3, \hat{p}_3 = 1$; and $H(8, 8, 6)$ by $p_1 = 3, p_2 = 3, p_3 = 5$. Note that in these three cases steps p_1 and \hat{p}_3 do

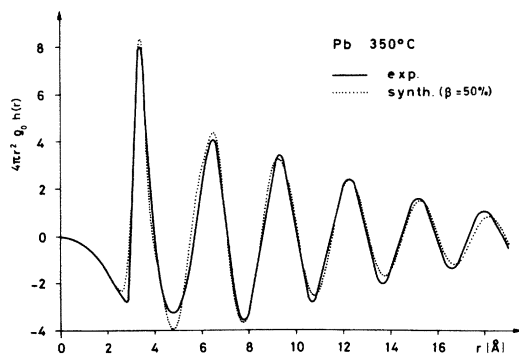


FIG. 2. RDF_{exp} calculated from the measured intensity of Pb at 350°C and $\text{RDF}_{\text{synth}}$ synthesized with a paracrystalline convolution polynomial.

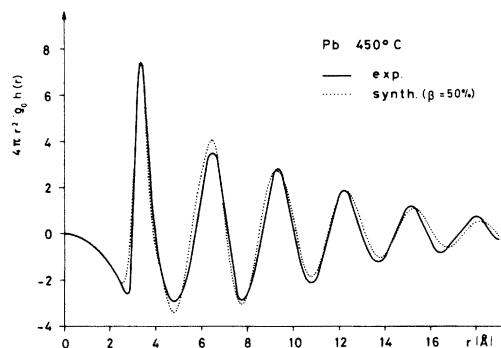


FIG. 3. RDF similar to Fig. 2 at 450°C.

not appear together because they must be replaced by p_2 steps according to Eq. (13).

III. APPLICATION TO LIQUID LEAD

The experimental radial distribution functions (RDF) we used were those of Steffen.¹² These curves show an asymmetrical first maximum whose asymmetry increases with increasing temperature (Figs. 2–4). One can expect therefore that the radial projection of the nearest-neighbors coordination statistic must be asymmetrical. We chose for the nearest-neighbors coordination statistic $H(r)$ a bimodal statistic, shown in Fig. 5,

$$H(\vec{r}) = (1 - \beta) H_I(\vec{r}) + \beta H_{II}(\vec{r}), \quad (14)$$

$$\langle \vec{r}_n \rangle = \int \vec{r} H_n(\vec{r}) d^3r, \quad \langle \vec{r}_I \rangle < \langle \vec{r}_{II} \rangle.$$

Gaussian distributions were chosen because their folding products are again Gaussian functions whose widths are given by the root of the quadratic sum of the two original distributions. Thus the convolution products can be calculated more easily. Since the fundamental statistics $H(\vec{r})$ each consist of two parts, Eq. (6) will be a convolution polynomial consisting of weighted Gaussian distributions whose radial widths (standard deviations) can be calculated by quadratic additions of the widths of the fundamental statistics in the direction UVW .

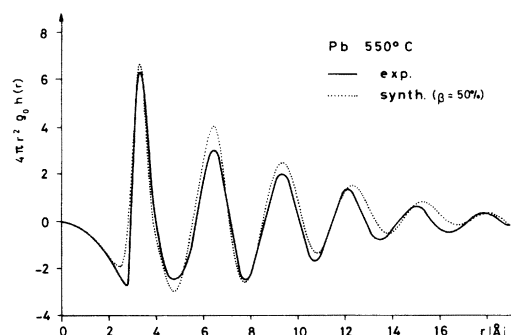


FIG. 4. RDF similar to Fig. 2 at 550°C.

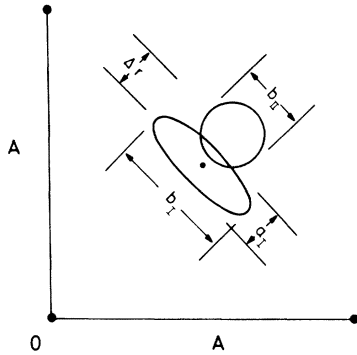


FIG. 5. Six parametric bimodal coordination statistics of Eqs. (10) and (11), schematically.

If a is, according to Fig. 5, the width of a three-axial Gaussian distribution at position 110 in the $[110]$ direction (x_1), b is the width in the $[\bar{1}10]$ direction (x_2), and c is the width in the $[001]$ direction (x_3), the statistic is given by

$$H(\vec{r} + \vec{r}) = [(2\pi)^{3/2} abc]^{-1} \times \exp -\frac{1}{2} [(x_1/a)^2 + (x_2/b)^2 + (x_3/c)^2]. \quad (15)$$

The width Δ in the direction $[UVW]$ is

$$\Delta^2 = (1/2R)^2 [(a^2 + b^2)(U^2 + V^2) + 2(a^2 - b^2)UV + 2c^2W^2], \quad R^2 = U^2 + V^2 + W^2, \quad (16)$$

by analogy with the fundamental calculations of Vogel,¹³ who used three-dimensional calculations to describe the paracrystalline distortions in solid $\text{Mn}_x\text{Fe}_{3-x}\text{O}_4$. The trial-and-error fitting of the parameters leads to the results that $H_{II}(\vec{r})$ [the second part of the fundamental statistic in Eq. (10)]

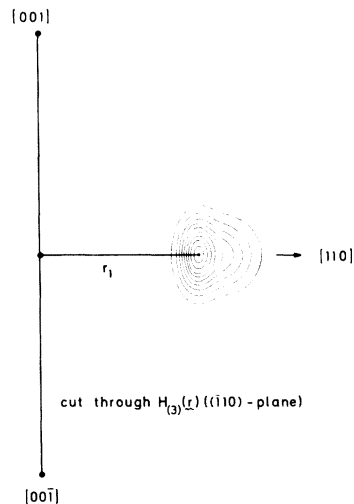


FIG. 6. Coordination statistic in the (110) plane. Each contour line corresponds to $0.05 \text{ atoms } \text{\AA}^{-3}$. The maximum value is therefore 0.45 \AA^{-3} .

TABLE I. Statistical parameters of the structure of lead below and above the melting point.

T ($^{\circ}\text{C}$)	325	350	450	550
r_I (\AA)	3.54	3.30	3.29	3.29
r_0 (\AA)	3.54	3.55	3.55	3.55
Δr (\AA)	0	0.50	0.53	0.56
β (%)	0	~ 50	~ 50	~ 50
a_I (\AA)	0.29	0.23	0.26	0.28
b_I (\AA)	0.29	0.82	0.88	0.93
c_I (\AA)	0.29	0.51	0.56	0.58
a_{II} (\AA)	...	0.51	0.56	0.58
K	12	11.6	11.5	11.3
ρ_0 (\AA^{-3})	0.0321	0.031	0.0306	0.0301

can be spherical symmetrical, while $H_I(\vec{r})$ (the first part of the statistic) has to be a three-axial Gaussian. One finds that a good approximation is

$$a_I < a_{II} \sim b_{II} \sim c_{II} \sim c_I < b_I. \quad (17)$$

The parameters which give the best fit to the experimental curves are shown in Table I (see Sec. II). $r_0 = r_I + \beta\Delta r$ is the position of the center of gravity of the fundamental statistic, $\Delta r = r_{II} - r_I$, and ρ_0 is the mean number density and K is the coordination number of nearest neighbors. K' can be calculated from r_0 and ρ_0 by assuming that point defects are statistically distributed in the liquid [see Eq. (10)]:

$$\frac{1}{12}K = \rho_0 r_0^3 / \sqrt{2}, \quad \rho_0 = \sigma L / A, \quad (18)$$

σ ($g \text{ cm}^{-3}$) is the macroscopic density, L is the Lohschmit-Avogadro number, and $A(g)$ is the atomic weight. The corresponding values for solid lead at 325°C are taken from Kaplow *et al.*¹⁴ The quality of the fit can be seen from Figs. 2-4. The positions of the first and second maxima and their profile are correctly described. The overall coincidence between the synthesized and the experimental radial distribution curve at 350°C is satisfying. The small differences at higher temperatures are due to the Gaussian approximation of the statistics. Figures 6 and 7 show two original cuts of the fundamental statistic $H(\vec{r})$ of liquid lead at 350°C . One can see contour lines of the frequency distribution starting at $\rho = 0.05 \text{ \AA}^{-3}$ and increasing in steps of 0.05 \AA^{-3} up to a maximum value of 0.45 \AA^{-3} .

IV. DISCUSSION

The first striking result of this work is that the mean distance r_0 between nearest neighbors does not change at the melting point but stays constant up to 550°C . The volume leap is produced by an abrupt decrease of the coordination number from 12 to 11.6 ± 0.2 (Table I). In the melt K' decreases at the rate of about 0.1 per 100°C .

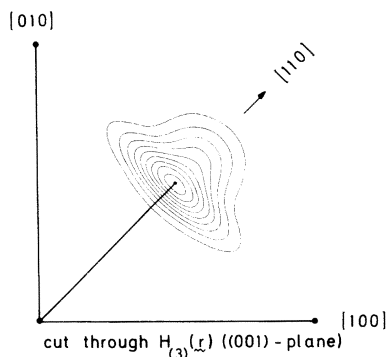


FIG. 7. As in Fig. 6, but in the (001) plane.

From this we deduce that at the melting point a rapid generation of point defects takes place. These vacancies can be Schottky defects, which produce a remarkable free volume. An expansion of the lattice constant does not take place.

The coordination statistic H splits according to Eq. (14) into two parts of the melting point, each with the weight $\beta \cong 0.5 \cong (1 - \beta)$ and mean values r_I and $r_I + \Delta r$, where $\Delta r = 0.5 \text{ \AA}$ (Table I). This can be interpreted by assuming that the melt consists of clusters (particles or microparacrystallites) which are separated by Δr (the difference between interparticle and intraparticle distances). Since H_I and H_{II} have the same weight, such a particle should consist on the average, of ~ 13 atoms, as schematically shown in Fig. 8. One can easily see that in such a microparacrystal the ratio of interparticle and intraparticle distances is about 1.

The partial statistics (H_I) with the smaller mean distance $r_I = 3.30 \text{ \AA}$ (Table I) can be explained by many Frenkel defects, which are produced together with Schottky defects.¹⁵ The interstitial atoms which result may be the reason why $r_I < r_0$ [Eq. (14)]. Thus for a certain number of atoms

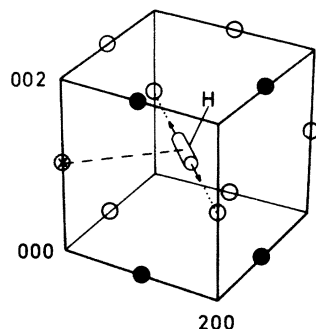


FIG. 8. Reference atom at 001 and the coordination statistic H of its neighbor 111 (schematically). The four black atoms hinder the diffusion of vacancies.

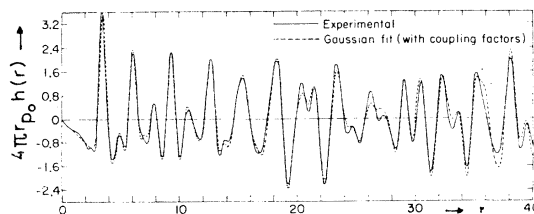


FIG. 9. Radial distribution function of Pb at 325 °C (below the melting point) (after Kaplow *et al.*, Ref. 7).

the coordination number is larger than 12 and the number of vacancies is larger than $[(12 - 11.6)/12] \times 100 = 3.3 \pm 1.6\%$.

From the radial distribution function at 325 °C (Fig. 9) one obtains a peak at $r_0 = 3.54 \text{ \AA}$ with the width $a_I = 0.29 \text{ \AA}$ (Table I) and a height $4\pi r_0 \rho_0 \times h(r_0) = 3.37 \text{ \AA}^{-2}$. Assuming that the peak of 325 °C is globular ($a_I = b_I = c_I$) one has to divide $4\pi r_0^2 \rho_0 g(r_0)$ by $2\pi a_I^2$ and by the coordination number 12 to obtain the three-dimensional peak value 2.75 \AA^{-3} of the coordination statistic. This is only six times larger than in the melt at 350 °C (0.45 \AA^{-3}) (Figs. 6 and 7). The neighboring atoms in the crystal are gathered in a globular volume with a diameter of $2a_I = 0.58 \text{ \AA}$ and spread out at the melting point to a volume which is only six times larger. This picture is quite different from that of conventional theories which discuss according to Eq. (11) a spherically symmetric first-neighbor statistic at 350 °C. The atoms are spread out to a 32-times-larger volume at the melting point, because $\rho_0 g$ has a peak value of only 0.085 \AA^{-3} , which comes from the first maximum of $4\pi r_0^2 \rho_0 h(r_0) \text{ \AA}^{-1}$ (Fig. 2) by dividing through by $4\pi r_0^2$ and adding the value of ρ_0 from Table I ($g = h + 1$).

In the real three-dimensional structure the atomic density $\rho(r)$ is not distributed uniformly in all directions. It is concentrated into the 12 next-neighbor coordination statistics, which have six-times-larger maxima than the over-all smeared spherically symmetric radial distribution function.

The shape of the coordination statistic $H(r)$ strongly suggests that atoms creep to interstitial places. If these lie adjacent to the reference atom then the shape of H_I suggests that this displacement takes place mainly in the tangential direction and predominantly in the face-diagonal direction ($b_I > c_I$; see Table I).

The statistics H_{II} suggests that about 50% of the distances belong to atoms in grain boundaries or half-dislocation lines of kink blocks. The width of H_{II} is a_{II} and within experimental error is the same in all directions and larger than a_I . Thus to a first approximation H_I describes the intraparticle distances and H_{II} describes the inter-

particle nearest-neighbor distances (as explained above).

The diffusion of single vacancies and interstitial atoms within the microdomains is indicated by the bimodal character of H . Six motions have in common the fact that the distance to the reference atom remains small. They therefore contribute to the statistics H_I . The neighbor 111 of the reference atom at 001 has two preferred direct neighbors 201 and 021 in the tangential plane. If displacements would occur only here H would have a rodlike shape, as drawn schematically in Fig. 8. The diffusion of a vacancy from the four other neighbors 102, 012, 100, and 010 to 111 takes place, but the reference atom 001 is then slightly repulsed.

The diffusion of vacancies can also happen from the five sites 210, 120, 221, 212, and 122. Now the distance from the migrating atom to the atom 001 increases and a contribution to H_{II} takes place. Kaplow *et al.*⁷ have discussed these kinds of displacements with reference to the melting point. They found that at the melting point the thermal oscillations of the four black atoms in Fig. 8 are so large that atom 111 can migrate in the direction $[1\bar{1}0]$ without being hindered by these, if they are in such extreme positions. Since the same holds for all other directions, the contribution of these motions to H must be rotationally symmetric with $b_I = c_I > a_I$. Alfrey¹⁶ has discussed such displacements in connection with liquid and amorphous structures.

A collective motion of the 12 neighbors of atom 111 within the first coordination shell gives rise to a rodlike contribution to H . As an example, the arrows in Fig. 10 indicate the cooperative displacements of the 12 atoms from a fcc position to an icosahedron. Inhibitions will happen only with the second coordination shell because it is impossible to build up a regular lattice with icosahed-

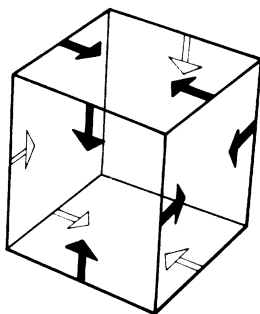


FIG. 10. Paracrystalline microdomain with the 12 next neighbors in fcc position. The arrows denote the displacement of a collective motion into the configuration of an icosahedron.

drons. Since at the melting point a certain amount of free volume is generated, such collective motions are possible in the first coordination shells.

A one-dimensional collective motion of atoms can explain a contribution to H_I and H_{II} , which is not rotational symmetric around the mean distance. The atom 111 tends to approach one of the six gaps in the first coordination shell at 110, 101, 011, 211, 121, or 112. If it is displaced, for example, in the direction $[0\bar{1}0]$ by d Å the reference atom 001 is repelled by the same amount in the direction $[\bar{1}00]$ of one of its next gaps. The relative motion of the atom 111 with respect to the atom 001 is then $\sqrt{2}d$ and points in the direction $[\bar{1}10]$ of the rod in Fig. 8. These gaps 101 and 011 therefore produce larger displacements than the two gaps at 110 and 112, where the reference atom is not repelled. These four motions together give a contribution to the statistics, H_I with $a_I < c_I < b_I$. The last two gaps at 211 and 121 give rise to motions which are not in a tangential direction and therefore produce larger distances, which contribute to the statistics H_{II} with $a_{II} > a_I$.

The motion described above (four paragraphs preceding) takes place in connection with the diffusion of vacancies. The motion considered in the paragraph just preceding this does not need any vacancies but requires that the four atoms of the next gap clear the way. This again is only possible by a collective motion of certain groups of atoms.

A two-dimensional collective motion exists in an fcc lattice according to Zhdanov¹⁷ for (111) slip planes in the $[\bar{1}10]$ direction. The atoms of adjacent slip planes then come into the so-called half-displacements or semidislocations.¹⁸ They contribute to the statistic H_{II} of the interparticle distances, but they will also contribute, to a certain amount, to the statistics H_I and nicely explain its special shape. For the reference atom 001 two slip planes exist with respect to the coordination statistics H in Fig. 8, namely the lattice planes (111) and $(1\bar{1}\bar{1})$. Each of them is inclined against the direction of the mean distance r_I of H , but the sum of their two statistics gives a tangential distribution with $a_I < c_I < b_I$.

A fundamental conclusion can be drawn from the three-dimensional structure analysis, namely, the conventional theories of liquids¹⁹ neglect the azimuthal dependence of the nearest-neighbor statistics and take into account only a simple r -dependence of the neighborhood of each arbitrarily chosen atom. These theories must therefore compensate for this neglected angular fluctuation by artificial radial fluctuations of spherically symmetric auxiliary functions. These have nothing in common with the physical state of the single microdomains. This holds for both the direct

correlation functions and the derived pair potentials, where the subsidiary maxima and minima of the latter and the large negative valley of the former¹⁸ have no physical significance.

ACKNOWLEDGMENT

We wish to thank Dr. Peter Bond for his help in formulating this work and for simulating discussions.

-
- ¹L. S. Ornstein and F. Zernike, Proc. Acad. Sci. Amsterdam 17, 793 (1914).
²L. E. Ballentine and J. C. Jones, J. Phys. A 51, 1831 (1973).
³H. D. Johnson, P. Hutchinson, and N. H. March, Proc. R. Soc. A 282, 283 (1964).
⁴D. M. North, J. E. Enderby, and P. A. Egelstaff, J. Phys. Chem. 1, 1 (1968).
⁵R. Hosemann, Z. Phys. 128, 465 (1950).
⁶R. Hosemann and S. N. Bagchi, *Direct Analysis of Diffraction by Matter* (North-Holland, Amsterdam, 1962).
⁷R. Kaplow, S. L. Strong and B. L. Averbach, Phys. Rev. 138, A1336 (1965).
⁸J. D. Bernal, Nature 185, 68 (1960).
⁹G. Willmann, dissertation (Freie Universität Berlin, 1971) (unpublished).
¹⁰R. Hosemann, G. Willmann, and B. Roessler, Phys. Rev. A 6, 2243 (1972).
¹¹R. Hosemann and K. Lemm, *Physics of Noncrystalline Solids* (North-Holland, Amsterdam, 1964).
¹²B. Steffen, dissertation (Freie Universität Berlin, 1974) (unpublished).
¹³W. Vogel, dissertation (Freie Universität Berlin, 1971) (unpublished).
¹⁴R. Kaplow, B. L. Averbach, and S. L. Strong, J. Phys. Chem. Solids 25, 1195 (1964).
¹⁵A. Seeger, Phys. 1, 1 (1955).
¹⁶Turner Alfrey, Jr., *Mechanical Behavior of High Polymers* (Interscience, New York, 1948).
¹⁷G. S. Zhdanov, *Crystal Physics* (Oliver and Boyd, Edinburgh, 1965).
¹⁸A. Seeger, Handb. Phys. 7, 2 (1958).
¹⁹H. N. V. Temperley, J. S. Rowlinson, and G. S. Rushbrooke, *Physics of Simple Liquids* (North-Holland, Amsterdam, 1968).